1969

Bearing capacity of concrete blocks or rock (69-1)

W. F. Chen

D. C. Drucker

EXPERIMENTAL STUDY OF THE BEARING CAPACITY OF CONCRETE BLOCKS

by

Michael W. Hyland

National Science Foundation Grant GY-4264 to Lehigh University for Undergraduate Research Participation.

Program Director
Dr. Lambert Tall

Project Supervisor
Dr. Wai-Fah Chen

Fritz Engineering Laboratory
Department of Civil Engineering
Lehigh University
Bethlehem, Pennsylvania

February 1969

TABLE OF CONTENTS

ABSTRACT

The applicability of the assumptions of perfect plasticity to punch loaded cylindrical concrete blocks is examined experimentally. The strain field is measured experimentally for punch loaded blocks with varying base conditions. The effects of block height, base friction, and a hole located directly under the loaded area on bearing capacity are investigated. Experimental results are compared with results of limit analysis solution by Chen and Drucker.[4,5]

1. INTRODUCTION

Quantitative understanding of concrete bearing capacity is necessary for design of many types of concrete members. The obvious example is a foundation structure; the end bearing zone of prestressed post-tensioned beams ~~are~~ is another. It is known that bearing capacity increases with the ratio of unloaded area to loaded area, to some upper limit. Present design methods are based on semi-empirical formulas and are considered by some to be overly conservative.[1,2]

Solutions of the problem based on the assumption of linear elastic behavior of the material have been presented[3]; however, this assumption does not hold true for concrete at loads near failure, where the stress-strain curve is non-linear. A stress-strain curve for a punch-loaded block (Fig. 1) indicates that near ultimate load the more highly stressed parts of a specimen are relieved by throwing stress to those regions of the specimen where stress is lower. Recently solutions presented by Chen and Drucker[4,5] assume concrete to behave in a prefectly plastic manner, allowing application of limit theorems of the generalized theory of perfect plasticity.[6] They have been successful in predicting failure loads.

Concrete normally exhibits brittle characteristics however, and the assumption of perfectly plastic behavior requires some degree of experimental verification in order to achieve credability. One of the purposes of this work is to attempt to provide this verification. In addition, the effect of base friction and specimen height on bearing capacity and the effect of a hole concentrically located under the loaded area are investigated. The results of experimental tests are compared with the predicted values, after Chen and Drucker.

2. PREVIOUS WORK

Previous load tests have been made; Meyerhof[7], Shelson[2], Au and Baird[8], and others have conducted tests on square blocks with various ratios of loaded area to surface area. Meyerhof and Shelson noted similarities in test results with results of triaxial compression tests, and developed rational expressions for predicting failure loads. Au and Baird investigated the problems associated with low ratios of surface area to loaded area, i.e. where the loading punch area approached more nearly the cross sectional area of the specimen. More recently, Hawkins[1] investigated the effects of eccentric loading and developed rational expressions for bearing capacity based on observed failure modes.

In previous investigations, the effect of block height was taken as negligible, unless the block was so short that the base interfered with the formation of a failure cone, and hence was not seriously investigated. Previous tests made no attempt to measure strain distribution throughout the specimen, while gross deflection has been considered[7]. The testing of a specimen with a hole directly under the loaded area again has never been undertaken. It was felt that this would give a close representation of actual conditions at the anchorage of tension steel in post-tensioned pre-stressed concrete members. Attempts have been made to quantify the effect of base friction on bearing capacity, and have determined some variation in load carrying capacity due to base friction, yet the effects of base conditions on strain distribution in concrete have not been previously investigated. Hence, to the best of the author's knowledge, these aspects of the overall bearing capacity problem were first investigated in the work reported here.

3. EXPERIMENTAL WORK

3.1 Specimens

The variables in specimen make-up and geometry are shown in Table 1. Two mixes were used because in previous investigations there had been some question as to the reliability of scaled down aggregate sizes as a means of making small scale tests more truly representative of larger structural applications. Punch diameter was varied as a means of changing the surface area: loaded area ratio; specimen diameter was constant at 6 in. The height of the cylinder was varied as it was felt to be an influencing factor in determining bearing capacity. Three different base conditions were used. A 7"·7"·3/8" steel plate was intended to provide high base friction. The "teflon" base and double-punch arrangements were intended to be friction-reducing. Their arrangements are shown in Fig. 1.

Concentrically located 5/8 in. diameter holes were used first to simulate actual condition around anchorage of post-tensioning rods; later as a means by which strain gages could be positioned in regions of greatest expected strain. Strain gages were employed in set 10 only; (Table 1) the positioning of gages is shown in Fig. 2.

Three specimens of each identical configuration were tested in order to minimize effects of inconsistent tests.

Four standard control cylinders were cast with each batch to be tested in compression, and in tension by the splitting tensile test (ASTM standard methods C 496).

3.2 Materials

Regular (Type 1) Portland cement was used in both mixes. The "mortar" mix was made with sand and cement only, while the concrete mix contained sand, cement, and 1/2 in. nominal crushed stone aggregate. The fineness modulus of sand was 2.74. The results of a sieve analysis are shown in Fig. 3.

The following mix ratios (by weight) were used in making the test specimens.

Mortar:

Water:	cement	1:	1.9
cement:	sand	1:	3.0

Concrete:

Water:	cement	1:	2.45
cement:	sand	1:	1.6
cement:	stone	1:	1.5

Each batch of materials was mixed in a rotary type mixer, and cast in accordance with A.S.T.M. Standard Methods C 192, except that cylinders shorter than 6 inches were filled with only two layers. The specimens with holes were cast with a steel pipe placed in the center of the mold and covered with grease to facilitate easy removal. The apparatus used is shown in Fig. 4.

3.3 Test Apparatus

The loading punches were made of tool steel 1 in. thick and 1.5 and 2.0 in. in diameter, all surfaces machined. They were centered by means of a masonite template. The testing machine used was a 300 kip capacity Baldwin hydraulic type, fitted with a spherical loading head. In the tests where no strain gages were used, the punches were placed concentrically over the hole in tests of specimens with holes in them. In the later tests with strain gages, punches were placed concentrically with respect to the cylinder. The maximum eccentricity of the hole in all tests was 1/4 in. from center. The loading punches were centered on the specimen in all tests of solid blocks, using the masonite templates.

The teflon thickness was chosen arbitrarily; at first a thickness of .003 in. was used, but was abandoned in favor of .005in. Thickness as the latter was not punctured during testing by grains of cement, sand, etc., as was the former. Plexiglas was chosen as a suitable plastic layer, following conclusions by Shah[9]. Strain gages used in the last set of tests were SR-4 Type A-X-5 with gage factors varying between 1.98 and 2.04. At first, a manually balancing type Baldwin recorder was used, but was later discarded in favor of an automatic digital recorder. Figure 5a shows a "teflon" base specimen with strain gages in position for testing.

In some early tests, one Ames dial gage was placed between the upper and lower platens of the testing machine in an attempt to find any qualitative differences in the load-deflection curves of "short" and tall cylinders, and "smooth" base and "rough" base cylinders. This arrangement is shown in Fig. 5b.

3.4 Test Procedure

One day after casting, molds were stripped from the specimens and specimens were placed in a 100% relative humidity curing room at about 75°F for four days; six days in tests where electric strain gages were employed. They were then placed in the atmosphere of the main lab to allow drying, in order to take advantage of the gain in strength due to drying. Most specimens were tested at about 7 days; set 10 was tested at about 34 days. The curing time was primarily determined by scheduling problems.

Load was applied at the approximate rate of 1 kip every 10 seconds, continuously until failure. Set 10 was loaded similarly, the loading being stopped and held approximately constant while strain gage readings were taken at two kip intervals. The time necessary to read all the gages was about one minute using the manually balancing recorder, and about 1/2 minute when using the digital recorder. When failure was impending the recording interval was reduced to 1 kip.

In tests where the teflon base was used, fresh pieces of teflon were used for each test. In placing the strain gages, each specimen was cleaned using first a commercial solvent, then acetone. Duco cement (solvent-release type) was used to attach gages to specimens. Interior gages were placed using an elastic rubber hose. The gage was attached to the outside of the hose, the hose inserted into the hole, and then inflated with air, forcing the gage against the inside cylinder wall. After each test, the exact position of each gage on the specimen was measured. This procedure resulted in a composite picture of strain distribution for both a smooth base and rough base specimen.

3.5 Accuracy of Results

Table 2 contains the average ultimate bearing pressure for all test configurations. The coefficients of variation are also given. In most cases the coefficient of variation was less than 10 percent. Table 3 gives the bearing pressure at failure divided by f'_c of the batch from which the respective specimens were made. This procedure is intended to eliminate variables introduced by differences in mixes and curing conditions. Every effort was made to keep test procedures uniform, but small variations in loading rate were unaviodable, as the valves of the testing machine were manually controlled.

The limits of physical measurement may have introduced errors that may have been more truly negligible had the scale of the tests been larger. It appears that these physical effects are dominant as an error source over recording errors. Many of these physical problems could be reduced or eliminated by enlarging the scale of the tests. For example, the magnitude of an error of 1/4 inch on a 6 inch specimen is twice the magnitude that would result from the same absolute error on a 12 inch specimen.

Strain gage readings are taken to be accurate within 3 percent. The "mortar" mix was chosen for the strain gage tests to eliminate the possibility of the gages "riding" a large piece of aggregate and hence not recording a representative strain in the material.

4. RESULTS

4.1 Effect of Friction on Bearing Capacity

Hansen, Nielsen, Kielland, and Thaulow[10] using data from tests by Thaulow[11], found that "reduction of height on the test specimen involves a significant increase in apparent strength provided friction is present on the test surface". They also state that by making the specimen height equal to twice the diameter, the friction effect can be practically eliminated. However, this information is the result of tests on specimens loaded over their entire surface and hence, cannot be directly compared with results of punch-loaded tests.

Qualitative comparisons can, however, be made. Note in Table 3, neglecting the double punch column, that in only two data sets out of six does the steel base specimen strength exceed that of the teflon base specimen of height 2 in., where the effect of friction is expected to be the greatest. This is seen again in Figs. 6 through 9. It is postulated that the weakening effect of the friction-reducing teflon-layer base was more than offset by the strengthening effect of the uniform bearing surface that was provided by the teflon-layer arrangement.

The idea that the effect of friction increases with decreasing specimen height was reinforced by results of the load-deflection curves from the dial-gage tests previously mentioned. Differences in behavior after first cracking were distinguished between "short" and "tall" specimens. Short specimens often achieved ultimate load well after large cracks were observed in the specimen. Typical load-deflection curves are shown in Figs. 10 and 11.

4.2 Modes of Failure

Two modes of failure were observed, "cone" formation and "column" formation combined with radial splitting. The formation of a column was only observed in 2 in. high specimens loaded with 2 in. punches. Both modes of failure were observed in specimens with and without the center hole, and in both type mixes. Cracks around the punch always spread radially outward, and were always separated by approximately equal angles. Failure modes are seen in Fig. 12.

4.3 Strain Distribution

Figure 13 shows the distribution of both horizontal and vertical strain along the central axis of a "composite" test specimen. Note that as depth from the loaded surface increases, the magnitude of the compressive strain decreases to a greater extent in the double punch specimen than in either the steel base or the teflon base specimen. The double punch specimen also has a greater region of horizontal tensile stress (hoop-type tension around perimeter of the hole) than does the steel base specimen, with the teflon base specimen about equalling the double punch specimen. This indication of greater distribution of tensile strain in teflon and double punch specimens coupled with the higher strength, suggests that first cracking, and hence, failure in the taller specimens where base friction is less of a factor, is controlled by the tensile strength of the material. This is also an indication of plastic redistribution of stress, supporting Chen and Drucker's assumptions[4,5].

Figure 14 illustrates horizontal distribution of vertical strain at the base of each type of specimen. The more uniform distribution of strain in double punch and teflon specimens again indicates plastic behavior. It may be argued that increased strengths are due primarily to the apparently more uniform stress distributions in teflon and double punch specimens. However the fact that failure always occured by a cone-formation splitting mechanism indicates that uniform stress distribution at the base causes small strength increases in comparison with the effect of increased distribution of tensile stress indicated by the tensile strain distribution. An assumed tensile stress distribution is seen in Fig. 15. It is believed that the tensile stress is first present in the region just below the failure cone. As load increases, the tensile stress is distributed throughout the specimen. Cracking occurs when ultimate tensile stress is reached, which occurs just under the failure cone.

4.4 Effect of Height on Bearing Capacity

Results indicate that increasing the height of the test specimen definitely increases the bearing capacity. However, it would be premature to attempt to quantify the effect from these tests. This phenomena is in accordance with the ideas mentioned above, as increased height yields increased capacity for distribution of tensile stress.

4.5 Comparison of Results with Solution of Chen and Drucker

The solution presented by Chen and Drucker is seen in Fig. 16. Predicted values are given in Table 3, and in Figs. 6 through 9. From these comparisons it is concluded that Chen and Drucker's solution gives an accurate upper bound for test results when H/2a is less than 2.0. For H/2a greater than 2.0, the discrepancy between predicted and observed values is too great to allow consideration of the predictions as being accurate. It would appear that up to some value for H/2a (the suggested value of 2.0 is arbitrary and is not part of Chen and Drucker's solution) the assumption of plastic behavior is valid. For greater values of H/2a the assumption is no longer valid and crack propogation dominates.

In computing failure loads from the equations of Chen and Drucker, the tensile strength of the material was taken as 1/12 of the standard cylinder compressive strength. This was done because of a report that the splitting tensile test yielded results which were approximately 30% too high.[12]

4.6 Effect of Concentrically Located Hole

Table 3 reveals that the effect of the centrally located hole is much smaller than would be expected if the compressive strength of concrete was assumed to control load carrying capacity. This observation again lends support to the idea that the tensile strength of the material governs failure, along with the specimen's ability to distribute tensile stress throughout its volume. According to this idea, since little material was removed, little change in test results should be expected. This is what was observed in tests.

5. CONCLUSIONS

From the results of this work some definite conclusions are evident, and the need for further study exists in some areas.

a. Friction effect.

Test results indicate that friction on the base of punch-loaded blocks causes no increase in their load carrying capacity. The difficulty in separating the effect of friction from the many things that might influence the specimen's load carrying capacity is great however, and this problem requires further investigation. Friction does appear to have some influence on strain distribution.

b. Strain Distribution and Ultimate Bearing Capacity.

The correlation of tensile strain distribution and ultimate bearing capacity indicates that maximum tensile stress is the governing factor in failure. The strain distribution is an indication of plastic stress distribution throughout the test specimen. However, further evidence is needed to reinforce these conclusions; notably with more complete instrumentation and a larger scale specimen.

c. Effect of Specimen Height on Ultimate Bearing Capacity.

There is a definite increase of ultimate strength with specimen height for punch-loaded blocks. Further tests are needed to quantify this effect.

e. Effect of Hole.

The results of tests on specimens with a 5/8" diameter centrally located hole reinforce the idea that failure is controlled by the attainment of ultimate tensile stress and that ability to distribute tensile stress throughout the specimen results in increased bearing capacity.

6. ACKNOWLEDGEMENTS

The work reported here was done under the National Science Foundation Undergraduate Research Participation Program, under direction of Assistant Professor W. F. Chen. The Program Director was Associate Professor Lambert Tall.

The author would like to thank Professors Chen and Hirst for their review of the manuscript, and the entire faculty and staff of Fritz Laboratory for their continual encouragement and assistance.

7. REFERENCES

1. Hawkins, N. M.
THE BEARING STRENGTH OF CONCRETE LOADED THROUGH RIGID PLATES, Magazine of Concrete Research Vol. 20, No. 2, March 1968, pp. 31-40.

2. Shelson, William
BEARING CAPACITY OF CONCRETE, Journal of the American Concrete Institute, Vol. 29, No. 5, November 1957, Proceedings Vol. 54, pp. 405-414.

3. Guyon, Y.
CONTRAINTES DANS LES PIECES PRISMATIQUES SOUMISES A DES FORCES APPLIQUEES SUR LEURS BASES, A VOISINAGE DE CES BASES, Publications, International Association for Bridge and Structural Engineering (Zurich), Vol. XI, 1951, pp. 165-226.

4. Chen, W. F., and Drucker, D. C.
THE BEARING CAPACITY OF CONCRETE BLOCKS OR ROCK, Journal of the Engineering Mechanics Division, A.S.C.E., Vol. 95, No. EM2, April 1969, To Appear.

5. Chen, W. F.
ENTENSIBILITY OF CONCRETE OR ROCK AND THE THEOREMS OF LIMIT ANALYSIS, Lehigh University Institute of Research Publication, Fritz Engineering Laboratory Report No. 356.5, November, 1968.

6. Drucker, D. C., Prager, W., and Greenberg, H. J.
EXTENDED LIMIT DESIGN THEOREMS FOR CONTINUOUS MEDIA, Quarterly of Applied Mathematics, Vol. 9, 1952, pp. 381-389.

7. Meyerhof, G. G.
THE BEARING CAPACITY OF CONCRETE AND ROCK, Magazine of Concrete Research, April 1953, pp. 107-116.

8. Au, T. and Baird, D. L.
BEARING CAPACITY OF CONCRETE BLOCKS, Journal of the American Concrete Institute, March 1960, Title No. 56-48, pp. 868-879.

9. Shah, H. H.
STUDY OF SURFACE-FRICTION OF A CYLINDRICAL SPECIMEN, Masters Thesis, New Mexico State University, University Park, New Mexico, August, 1966.

10. Hansen, H., Kielland, A., Nielsen, K. E. C., and Thaulow, S.
COMPRESSIVE STRENGTH OF CONCRETE-CUBE OR CYLINDER?, RILEM Bulletin No. 17, December 1962, pp. 23-30.

11. Thaulow, S.
INNFLYTELSEN AV FRIKSJONEN I TRYKKFLATNE VED BESTEMMELSE AV BETONGENS TRYKKFASTHET MED PROVE-LEGMER AV FORSKJELLIG HOYDE, Nordisk Betong, Stockholm, nr. 4, 1960, pp. 321-24.

12. Kaplan, M. F.
STRAINS AND STRESSES OF CONCRETE AT INITIATION OF CRACKING AND NEAR FAILURE, Journal of the American Concrete Institute, Vol. 60, pp. 853-879, July 1963.

8. Tables and Figures

TABLE 1

SPECIMEN CONFIGURATION

Set	Make	Type	Punch Diameter (in.)	Cylinder Height (in.)	Number Tested: Steel Base	Number Tested: Teflon Base	Number Tested: Double Punch
1	MORTAR	SOLID	1.5	6	3	3	3
2				3	3	3	3
3				2	3	3	3
4			2.0	6	3	3	3
5				3	3	3	3
6				2	3	3	3
7		WITH HOLE	1.5	6	3	3	3
8				3	3	3	3
9				2	3	3	3
10*			2.0	6	4	4	4
11				6	3	3	3
12				3	3	3	3
13				2	3	3	3
14	CONCRETE	SOLID	1.5	6	3	3	3
15				3	3	3	3
16				2	3	3	3
17			2.0	6	3	3	3
18				3	3	3	3
19				2	3	3	3
20		WITH HOLE	1.5	6	3	0	3
21				3	3	0	3
22				2	3	0	3
23			2.0	6	3	0	3
24				3	3	0	3
25				2	3	0	3

*With Strain Gages at 34 days. (Total # = 210)

TABLE 2

Numerical Results & Coefficient of Variation

Set	Make	Type	Punch Dia.	Height in.	Ult. Bearing Pressure			Coef. Variation, %		
					Steel Base	Teflon Base	Double Punch	Steel Base	Teflon Base	Double Punch
1	MORTAR	SOLID	1.5	6	15,180	16,300	13,400	4.7	8.5	6.8
2				3	11,750	11,400	14,950	8.7	20.	5.1
3				2	9,140	9,830	11,620	3.0	9.4	3.8
4			2.0	6	8,260	9,440	9,300	6.2	4.7	<5
5				3	7,530	5,800	8,270	12.7	15.7	<5
6				2	8,840	6,570	7,220	3.2	6.7	8.3
7		WITH HOLE	1.5	6	16,090	16,400	17,150	<5	4.9	4.2
8				3	10,580	9,250	18,030	<5	20	2.3
9				2	8,980	8,460	13,770	50	7.8	4.3
10*			2.0	6	11,650	11,450	11,850	-	-	-
11				6	8,960	8,370	9,570	<5	5.0	<5
12				3	6,820	6,910	11,070	<5	6.8	8.2
13				2	5,400	5,950	7,330	11.7	15.8	12.4
14	CONCRETE	SOLID	1.5	6	12,200	12,970	20,650	4.7	10.1	<5
15				3	18,475	12,100	18,270	6.0	6.9	8.6
16				2	16,520	10,080	15,230	5.5	10.9	5.9
17			2.0	6	15,100	9,300	12,470	-	-	10.7
18				3	9,400	6,780	11,230	<5	10.6	10.8
19				2	8,380	5,810	9,300	2.4	<5	4.6
20		WITH HOLE	1.5	6	21,000	-	21,000	4.6	-	<5
21				3	16,300	-	20,400	<5	-	9.5
22				2	13,170	-	17,320	<5	-	<5
23			2.0	6	12,700	-	10,080	<5	-	<5
24				3	8,730	-	10,080	8.9	-	<5
25				2	7,400	-	10,300	9.1	-	<5

Ult. Bearing Pressure for Specimens with hole is given here as $P/(A_P - A_H)$; P=Load, A_P = Area Punch, A_H = Area Hole.

*Tested at about 34 days.

TABLE 3

Non-Dimensioned Results - Comparison With Predictions of Chen & Drucker.

Set	Make	Type	Punch Dia.	Height in.	Ult. Bearing Pressure/f'_c			Predicted by Chen & Drucker
					Steel Base	Teflon Base	Double Punch	
1	MORTAR	SOLID	1.5	6	2.98	3.71	3.04	5.70
2				3	2.30	2.59	3.40	3.45
3				2	1.80	2.23	2.63	2.78
4			2.0	6	1.62	2.14	2.18	3.76
5				3	1.48	1.59	1.93	2.38
6				2	1.73	1.49	1.68	1.88
7		WITH HOLE	1.5	6	2.96	2.88	3.28	5.70
8				3	1.95	1.62	3.56	3.45
9				2	1.49	1.49	2.72	2.78
10*			2.0	6	2.22	2.14	2.18	3.76
11				6	1.80	1.61	2.12	3.76
12				3	1.37	1.33	2.45	2.38
13				2	1.08	1.12	1.62	1.88
14	CONCRETE	SOLID	1.5	6	3.00	3.12	3.21	5.70
15				3	2.88	2.91	2.89	3.45
16				2	2.58	2.42	2.37	2.78
17			2.0	6	2.36	2.24	2.07	3.76
18				3	1.47	1.63	1.86	2.38
19				2	1.31	1.40	1.54	1.88
20		WITH HOLE	1.5	6	3.14		3.11	5.70
21				3	2.42	Not	3.03	3.45
22				2	1.97	Cast	2.57	2.78
23			2.0	6	2.08		1.55	3.76
24				3	1.43	Not	1.68	2.38
25				2	1.21	Cast	1.48	1.88

Ult. Bearing Pressure for Specimens with Hole is given here as $\frac{P}{A_P}$

P = Ult. Load

A_P = Punch Area

This is done to allow comparison with formula prediction by Chen & Drucker.

*Tested at about 34 days.

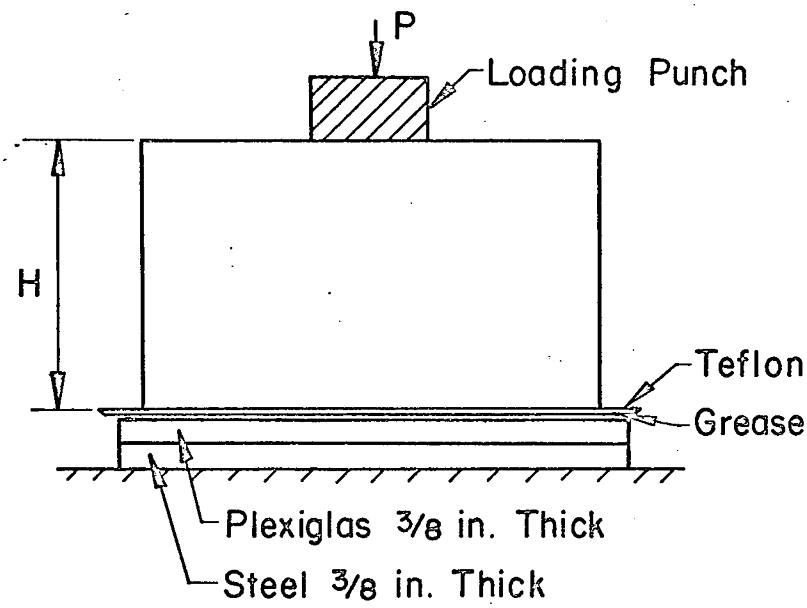

(a) Teflon Base Arrangement

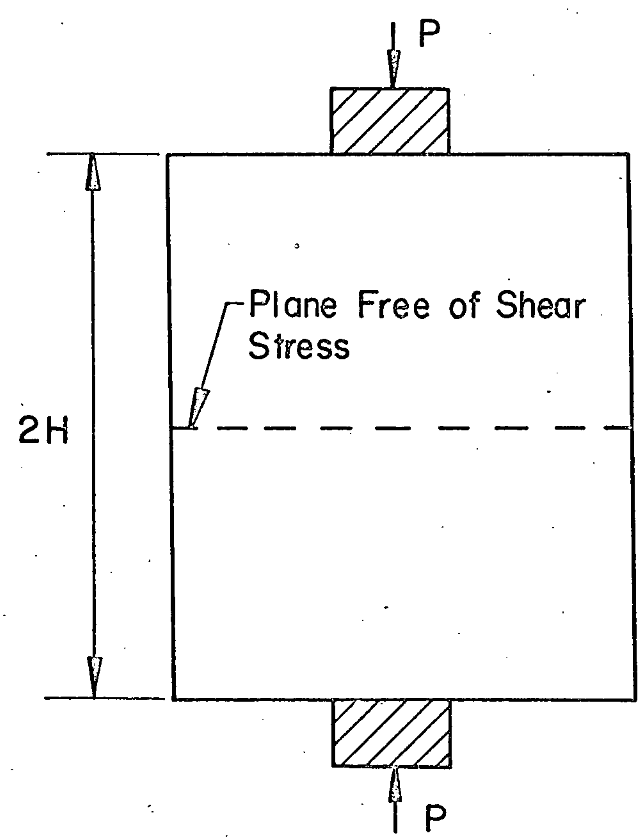

(b) Double Punch Arrangement

Fig. 1

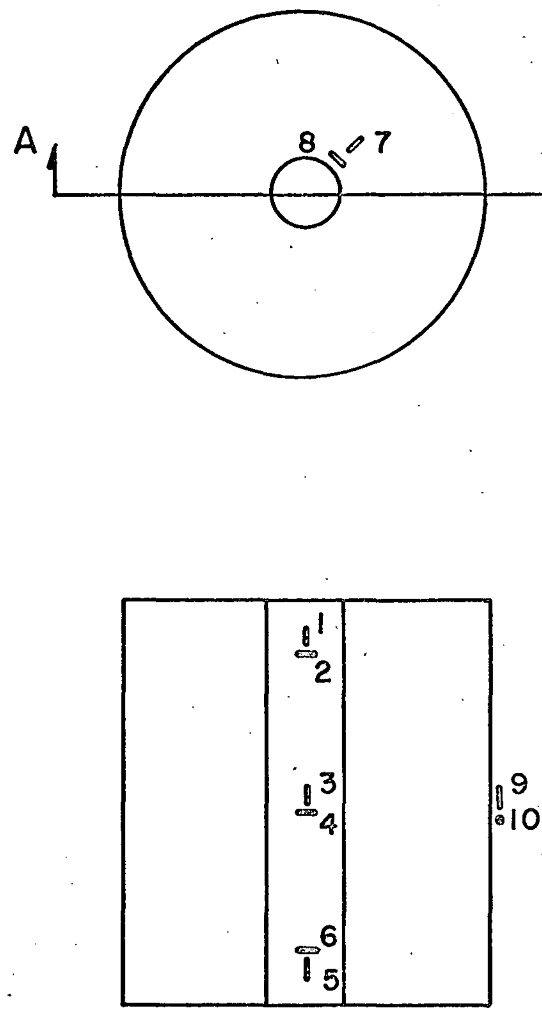

SEC. A-A

(Double Punch Arrangement-Set 10)

Fig. 2 Strain Gage Locations And Numbering System

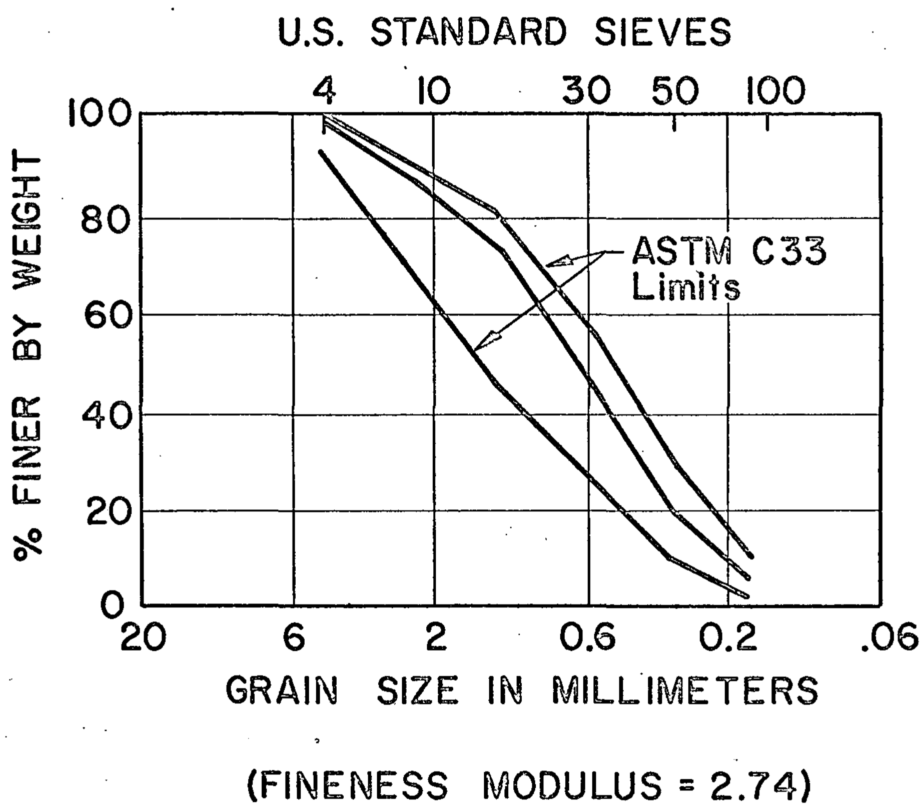

Fig. 3 Fine Aggregate Sieve Analysis

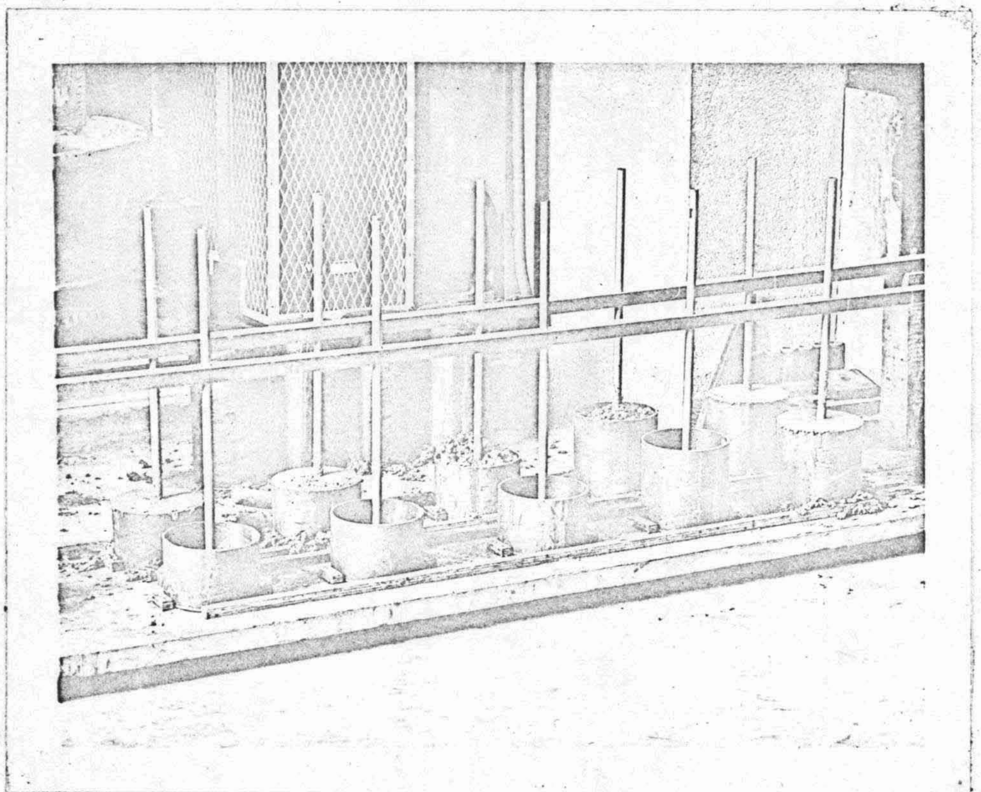

Fig. 4 Casting Apparatus Used in
Forming Specimens with Hole.

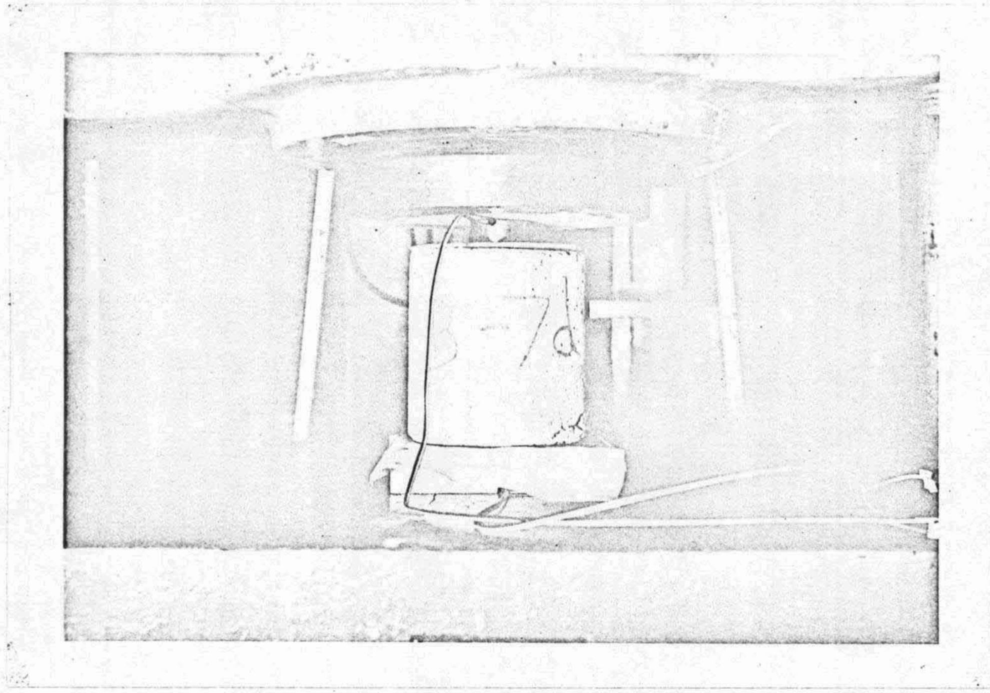

Fig. 5

a. "Teflon" Base Specimen with Strain gages ready for testing.

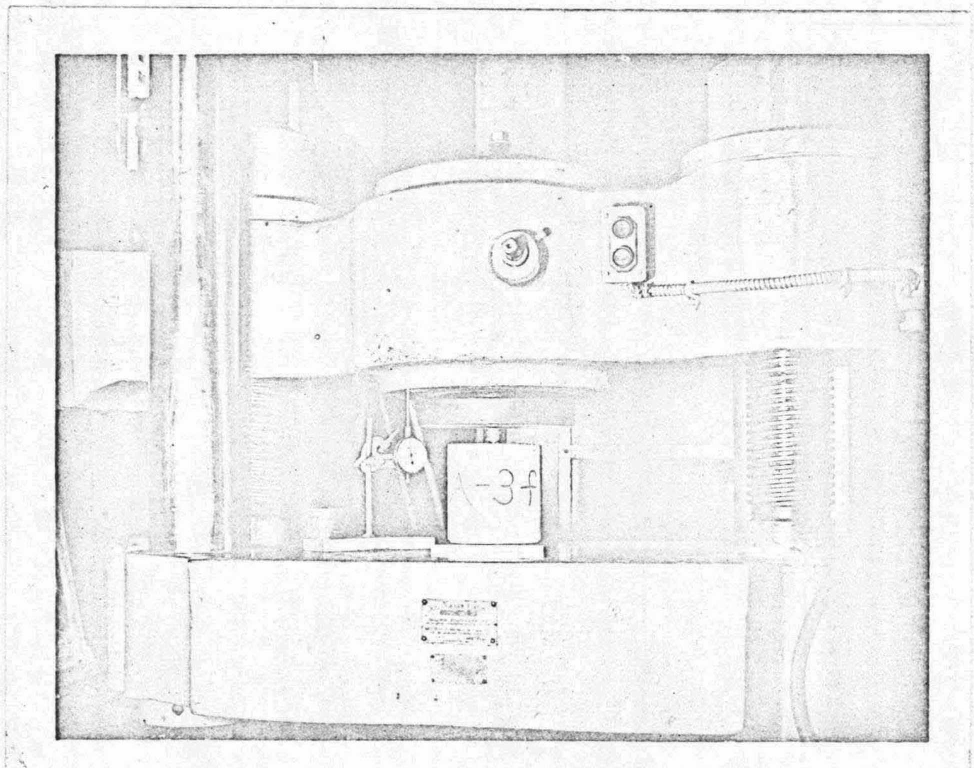

b. Dial gage arrangement. (Steel Base)

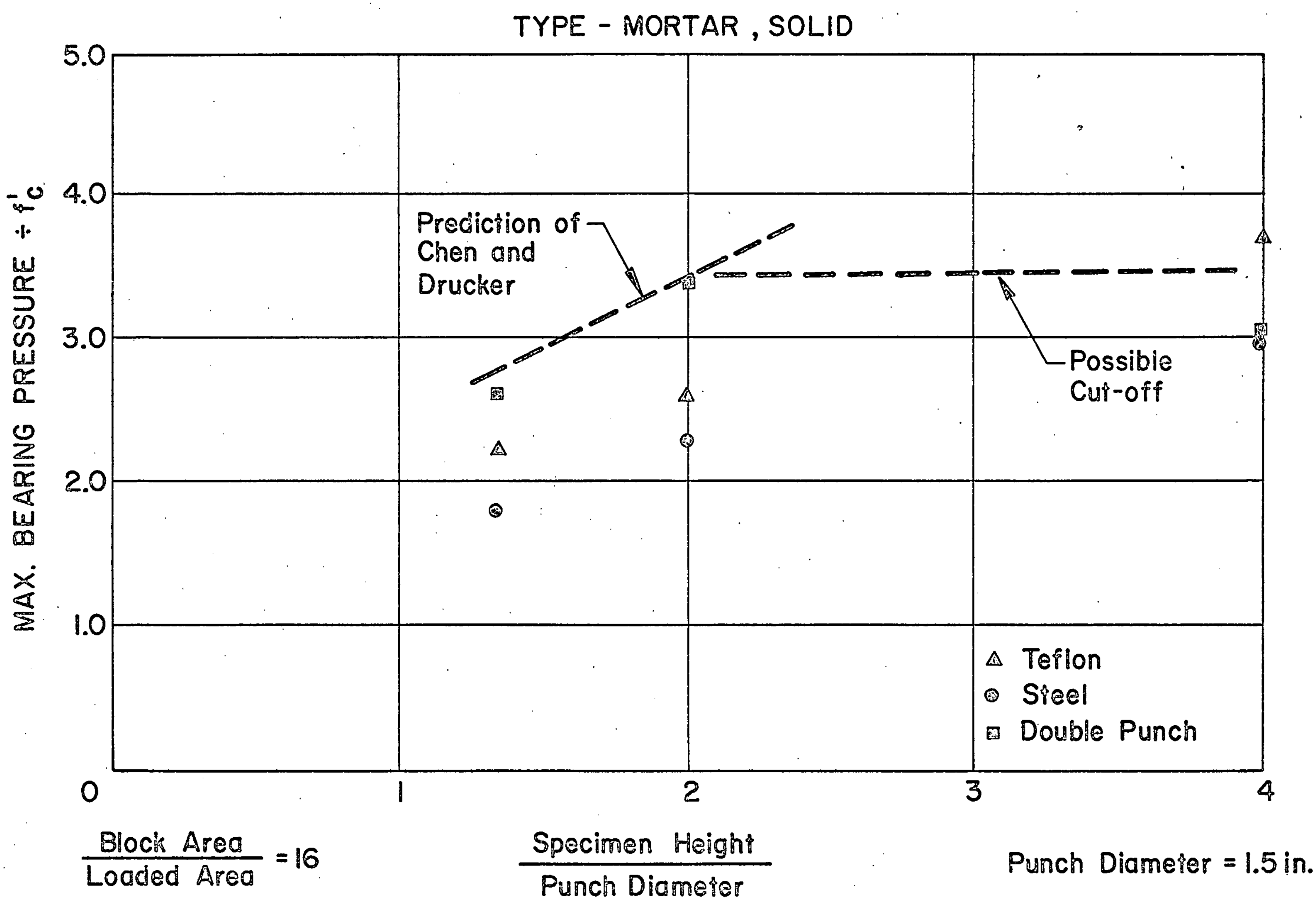
TYPE - MORTAR , SOLID
MAX. BEARING PRESSURE ÷ f'c
5.0
4.0
3.0
2.0
1.0
0
1
2
3
4
Prediction of Chen and Drucker
Possible Cut-off
Teflon
Steel
Double Punch
Block Area / Loaded Area = 16
Specimen Height / Punch Diameter
Punch Diameter = 1.5 in.

Fig. 6

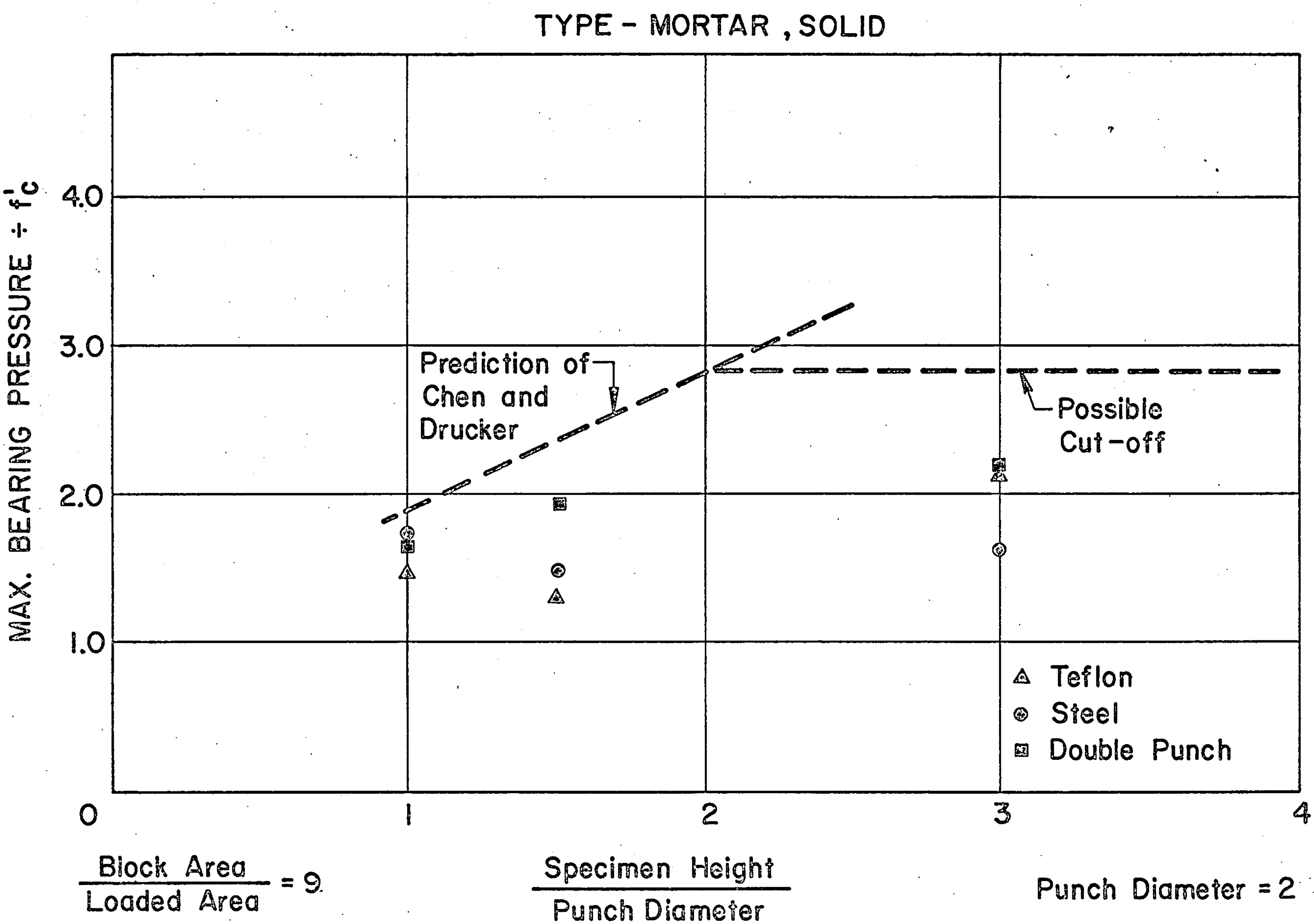

TYPE - MORTAR , SOLID
MAX. BEARING PRESSURE ÷ f'c
4.0
3.0
2.0
1.0
0
1
2
3
4
Prediction of Chen and Drucker
Possible Cut-off
Teflon
Steel
Double Punch
Block Area / Loaded Area = 9
Specimen Height / Punch Diameter
Punch Diameter = 2 in.

Fig. 7

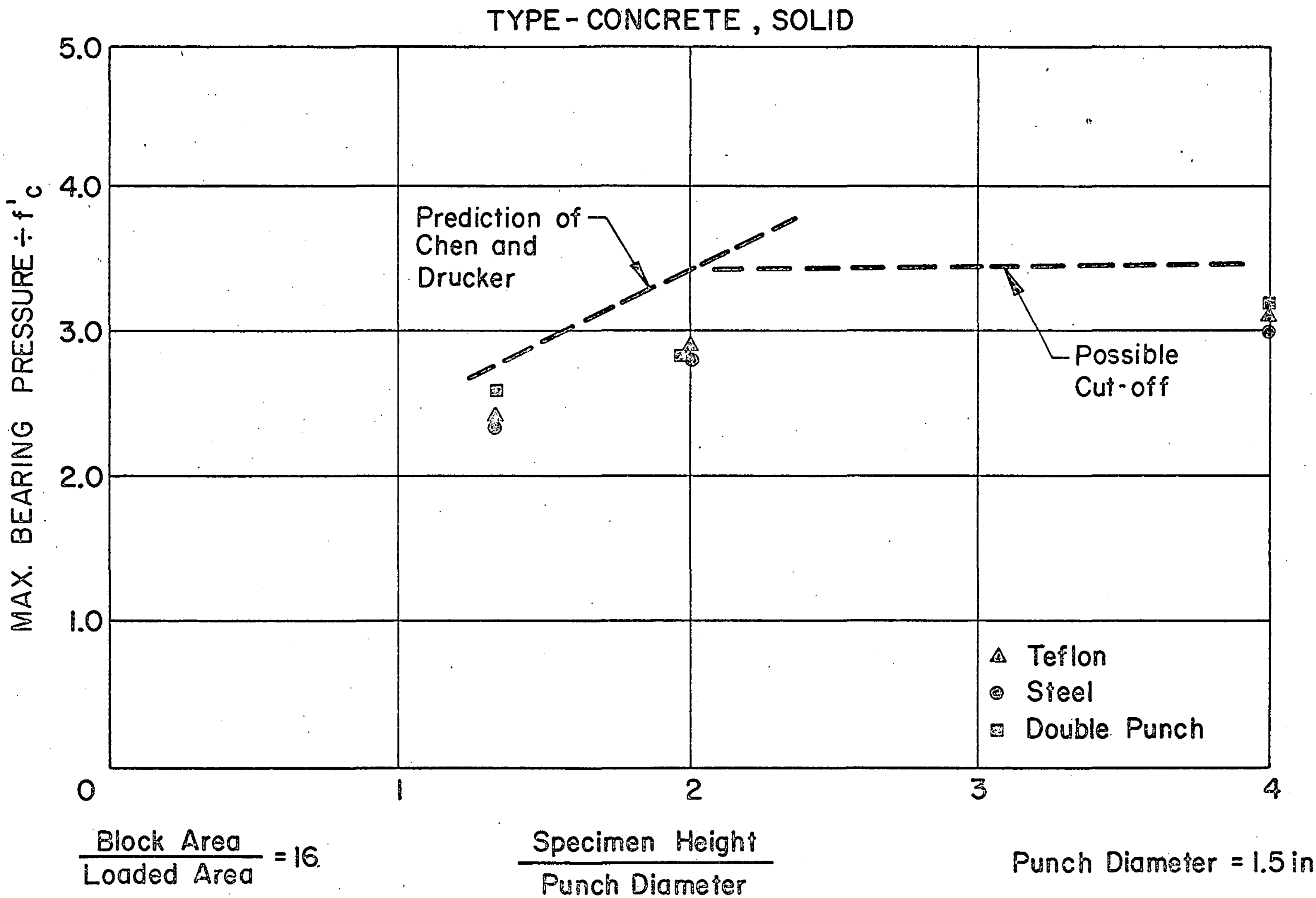
TYPE - CONCRETE , SOLID
MAX. BEARING PRESSURE ÷ f'c
5.0
4.0
3.0
2.0
1.0
0
1
2
3
4
Prediction of Chen and Drucker
Possible Cut-off
Teflon
Steel
Double Punch
Block Area / Loaded Area = 16
Specimen Height / Punch Diameter
Punch Diameter = 1.5 in.

Fig. 8

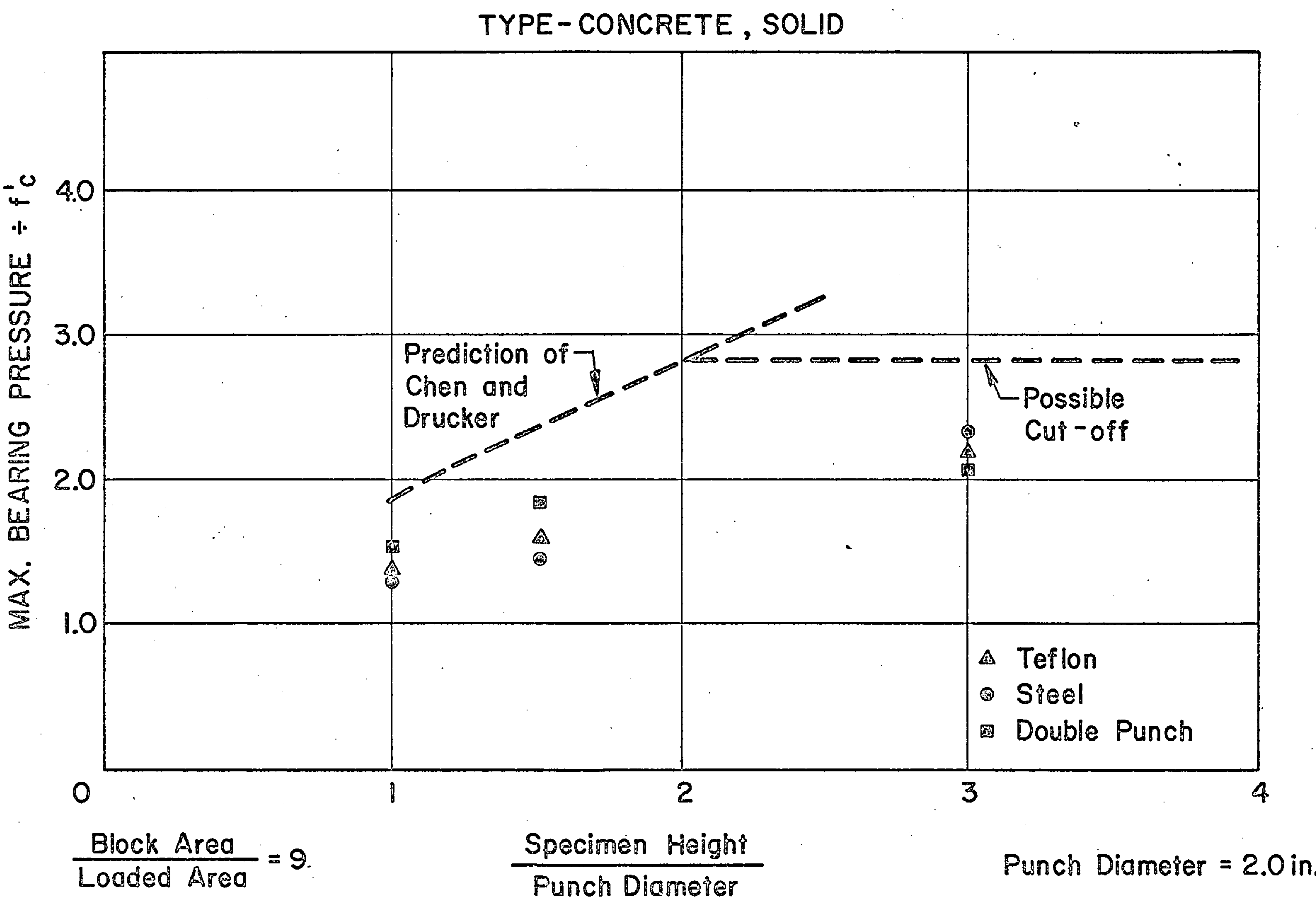
TYPE-CONCRETE, SOLID
MAX. BEARING PRESSURE ÷ f'c
4.0
3.0
2.0
1.0
0
1
2
3
4
Prediction of Chen and Drucker
Possible Cut-off
Teflon
Steel
Double Punch
Block Area / Loaded Area = 9
Specimen Height / Punch Diameter
Punch Diameter = 2.0 in.

Fig. 9

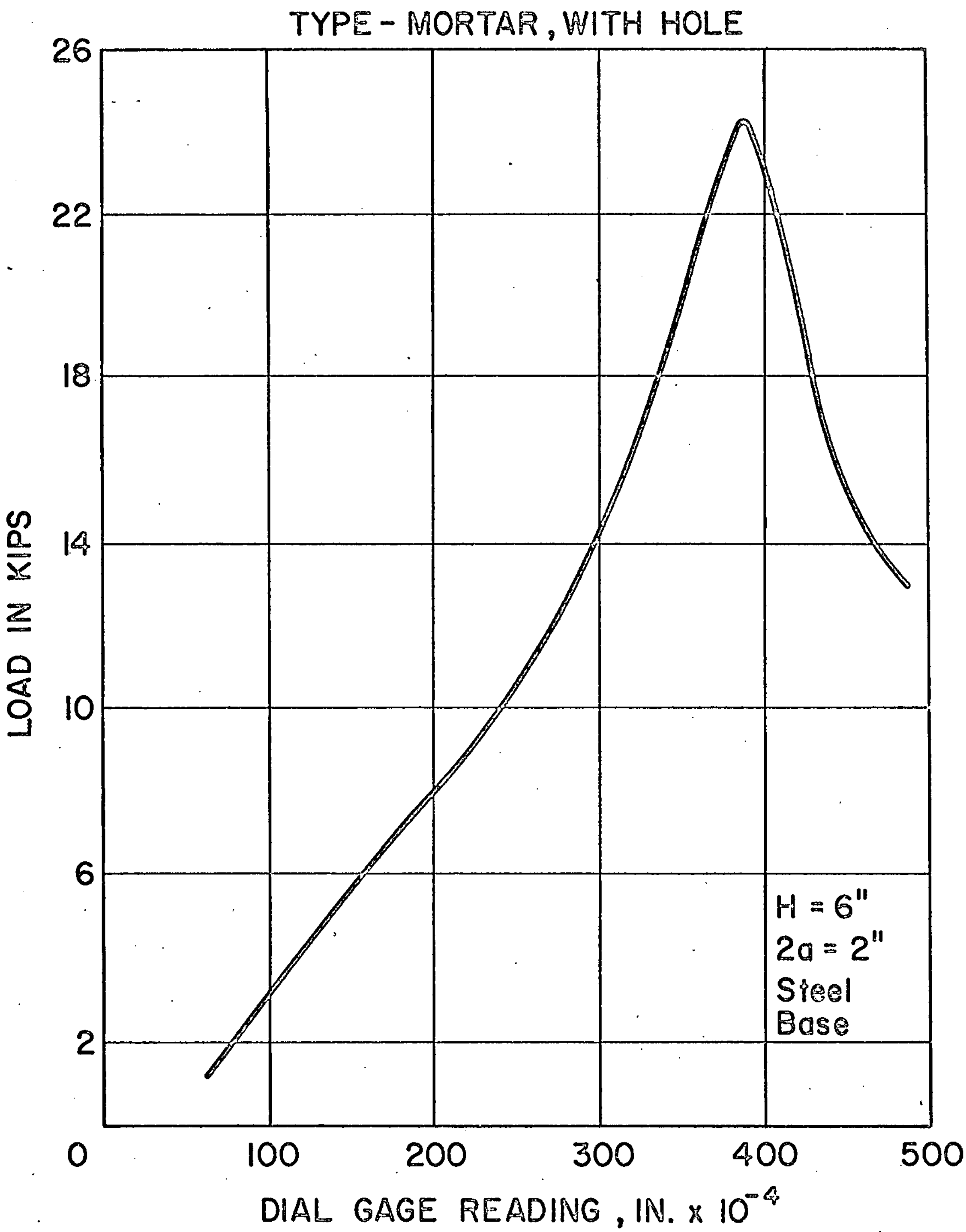

Fig. 10 Load-Deflection Curve For "Tall" Cylinder

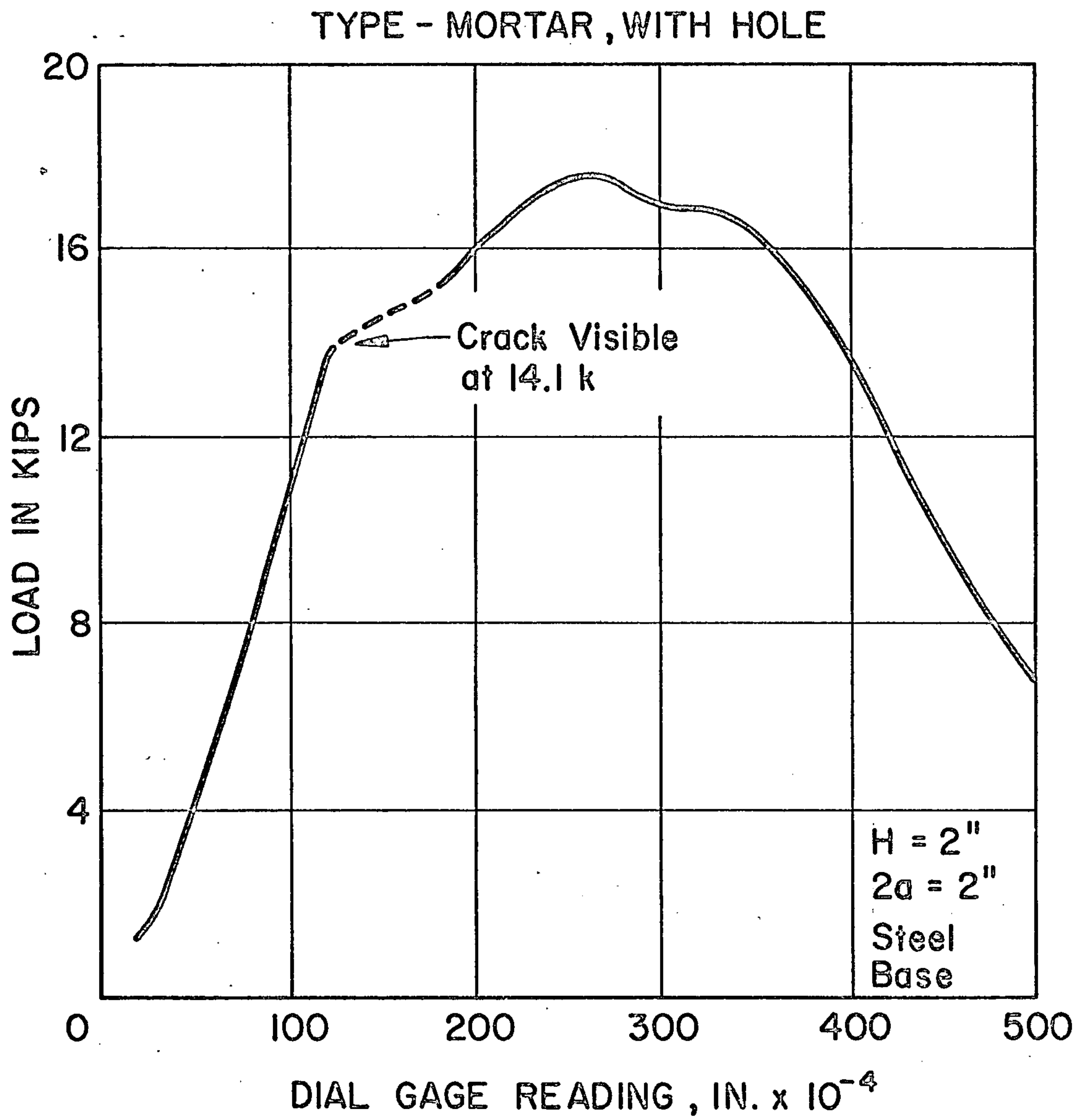

Fig. 11 Load-Deflection Curve For "Short" Cylinder

Fig. 12

Failure Modes

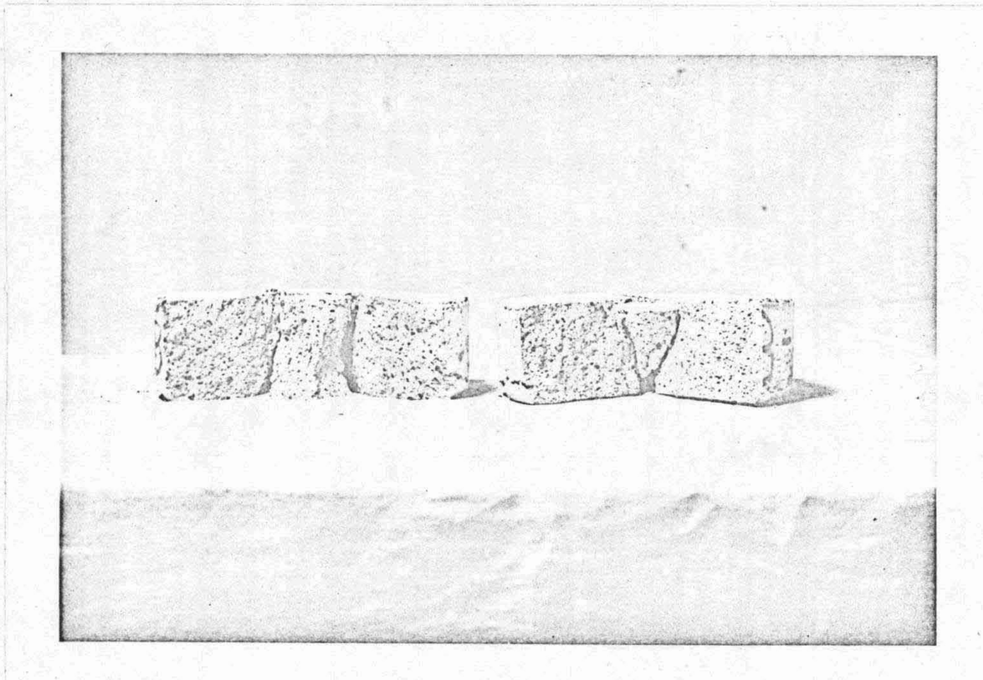

a. Cone (Left) and Column Formation

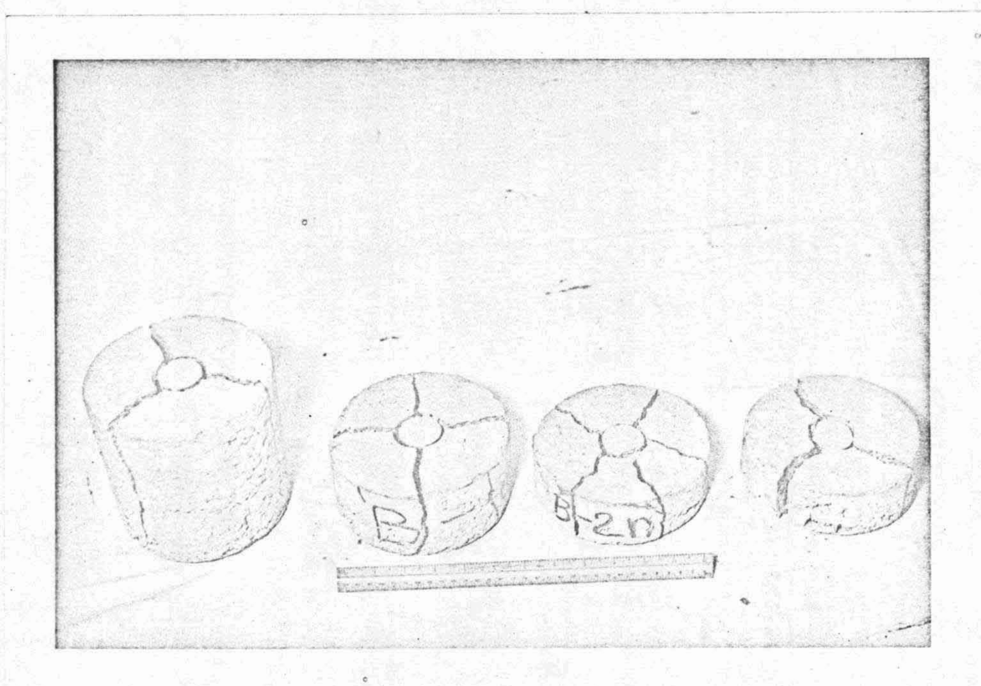

b. Radial Symmetry of Cracks

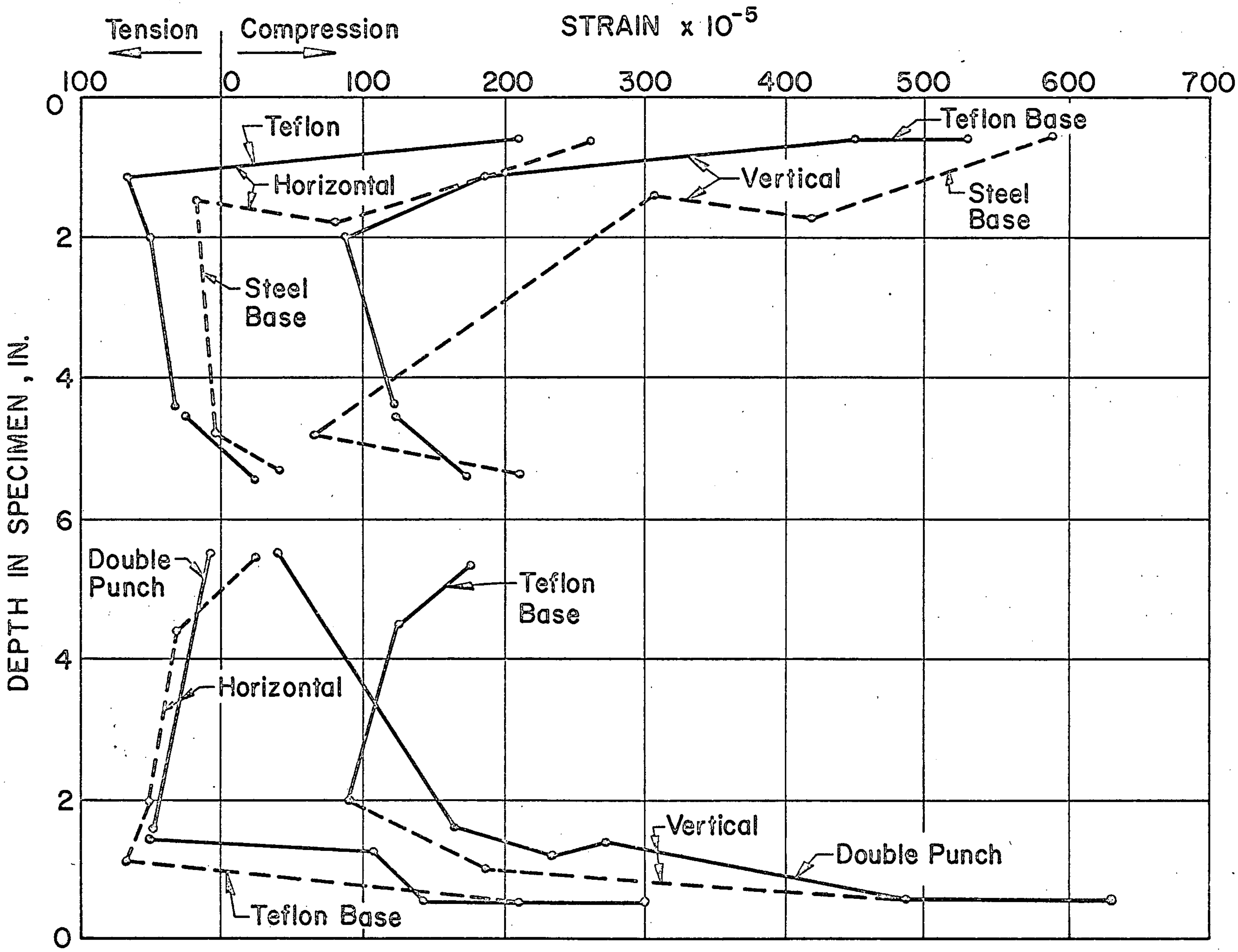

Fig. 13 Vertical And Horizontal Strain Distribution Along Central Axis

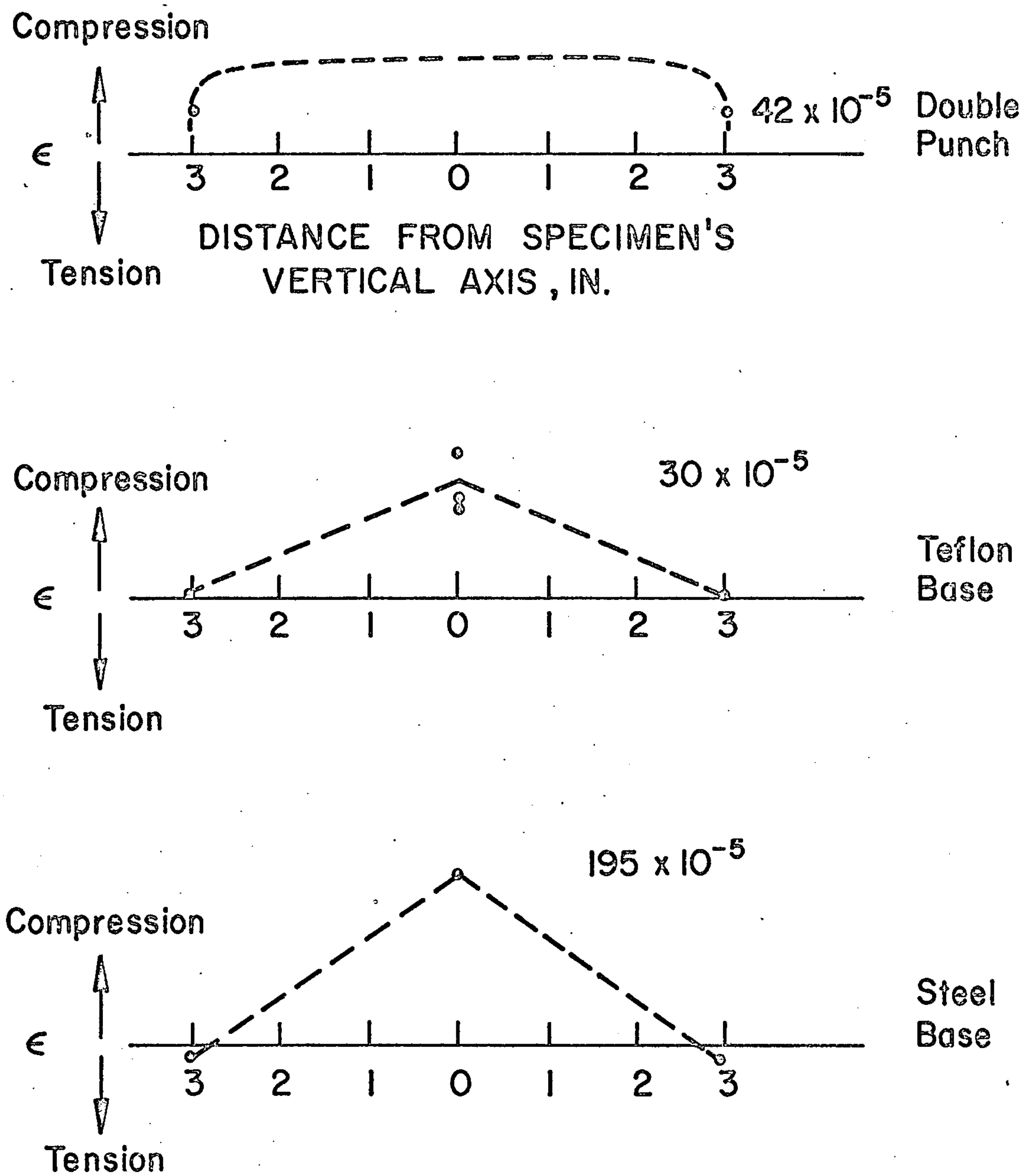

Fig. 14 Horizontal Distribution of Vertical Strain

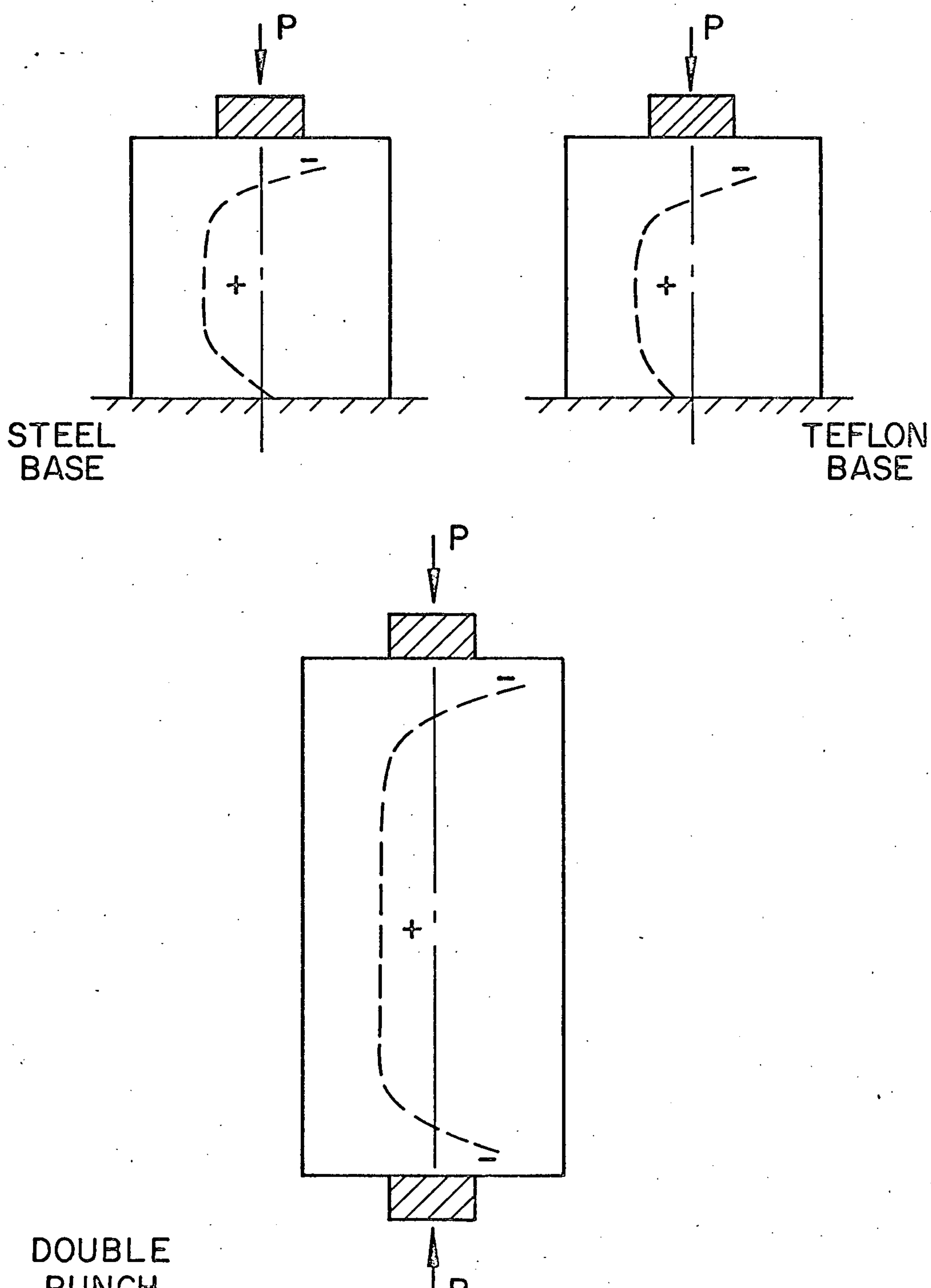

Fig. 15 A Possible Tensile Stress Distribution

Expression of Chen and Drucker [4]

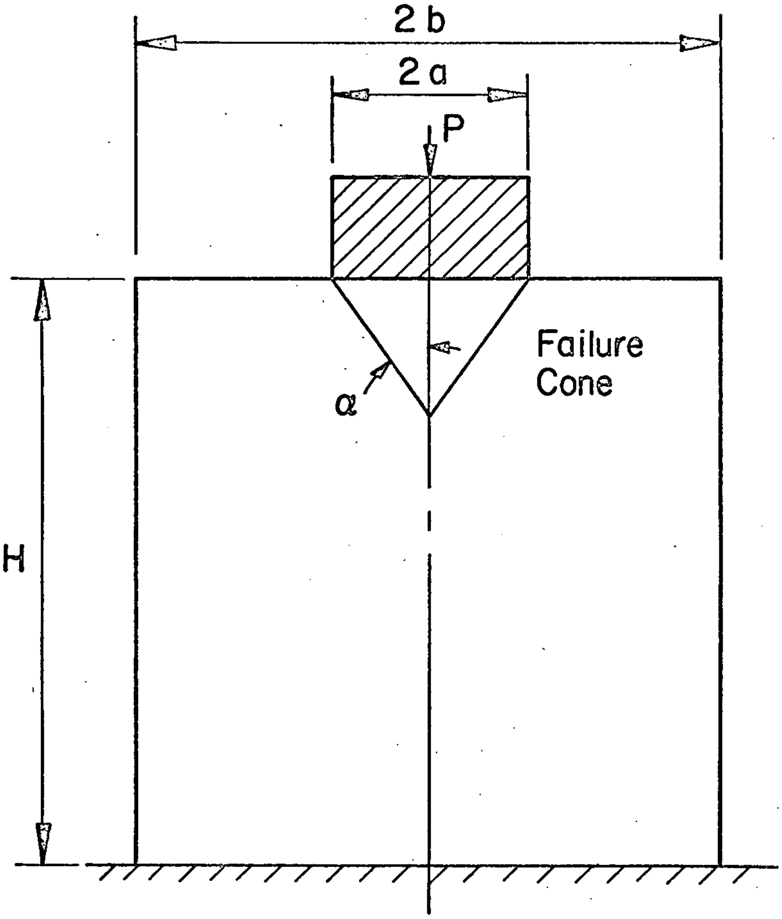

$$q_3 = f'_t \left[\frac{2bH}{a^2} \tan(2\alpha + \emptyset) - 1\right]$$

$$\alpha = \tan\emptyset + \sec\emptyset \left[1 + \frac{\frac{2bH}{a^2}}{\frac{f'_c}{f_t}\left(\frac{1-\sin\emptyset}{2}\right) - \sin\emptyset}\right]^{\frac{1}{2}}$$

$\emptyset$ = internal friction angle, assumed = 30°

f_t = tensile strength of material

f'_c = standard cylinder compressive strength

$q_3 = \frac{P}{\pi a^2} = \frac{\text{Load}}{\text{Punch Area}}$

Fig. 16